Cite this: DOI: 10.1039/xxxxxxxxxx

How carotenoid distortions may determine optical properties: Lessons from the Orange Carotenoid Protein: Supplementary Material

Tiejun Wei[a], Vytautas Balevičius Jr.[a], Tomás Polívka[b], Alexander V. Ruban[a] and Christopher D. P. Duffy[a,*]

[a] *School of Biological and Chemical Sciences, Queen Mary University of London, London E1 4NS.*
[b] *Institute of Physics and Biophysics, University of South Bohemia in Czech Republic, Czech Republic*
[*] Corresponding author: c.duffy@qmul.ac.uk

1 AM1-MECI orbital Active Space used for calculation of Ech excited states.

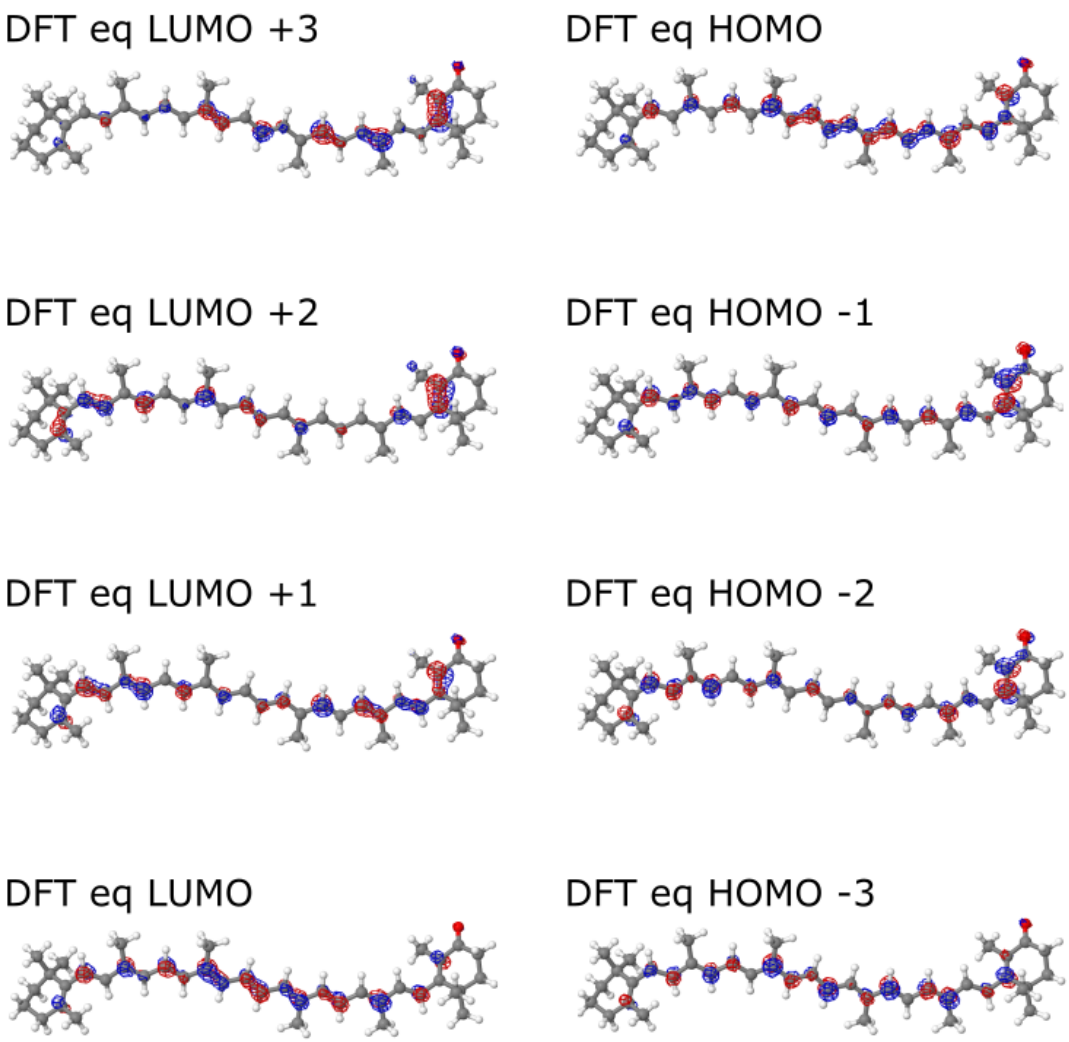

Fig. 1 Visualization of the AM1-MECI orbital active space calculated for the DFT equilibrium (*cis-cis*) structure of Ech.

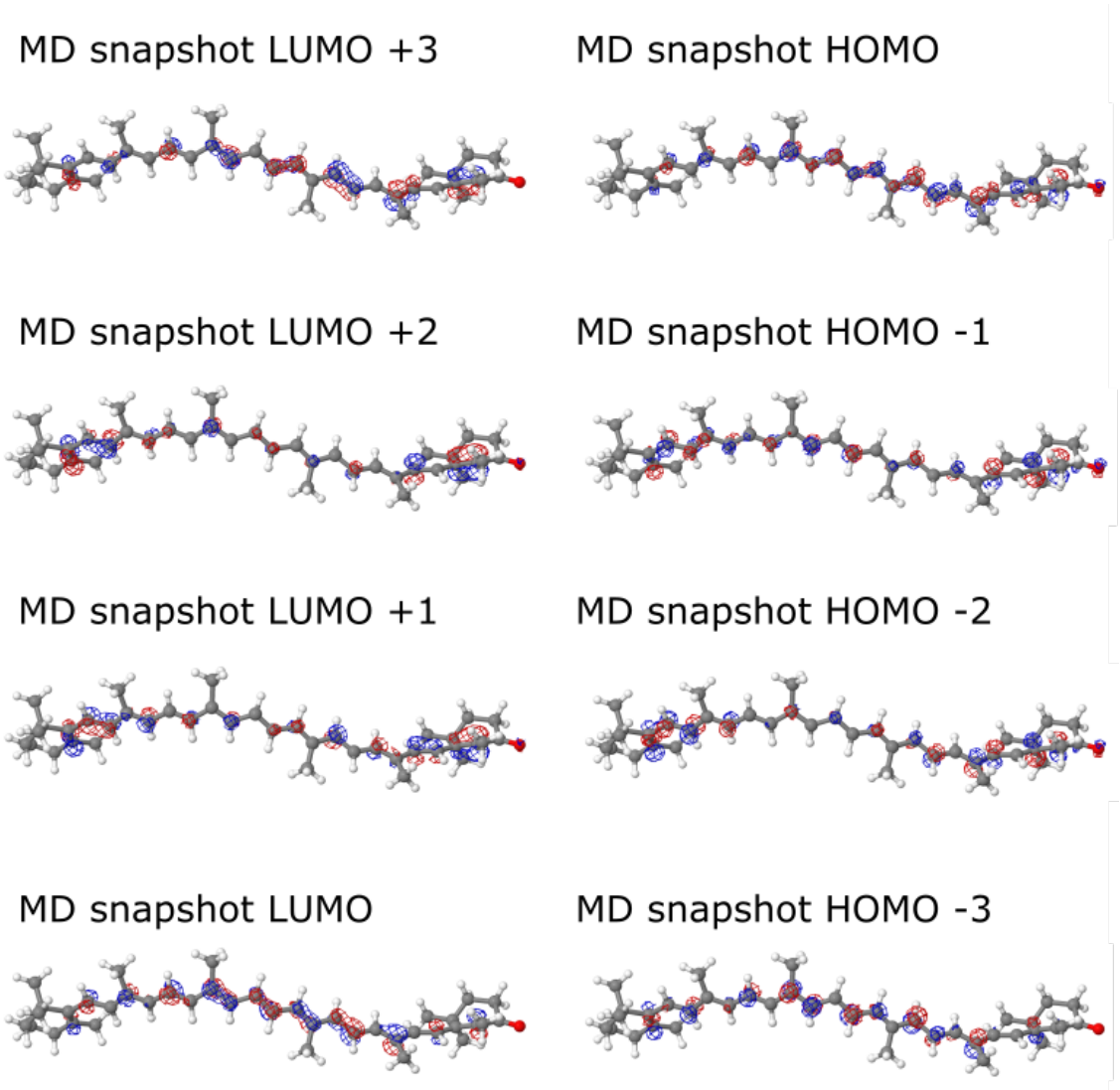

Fig. 2 Visualization the AM1-MECI active space calculated for a randomly-sampled snapshot of Ech in THF. It remains relatively unchanged with respect to the equilibrium structure.

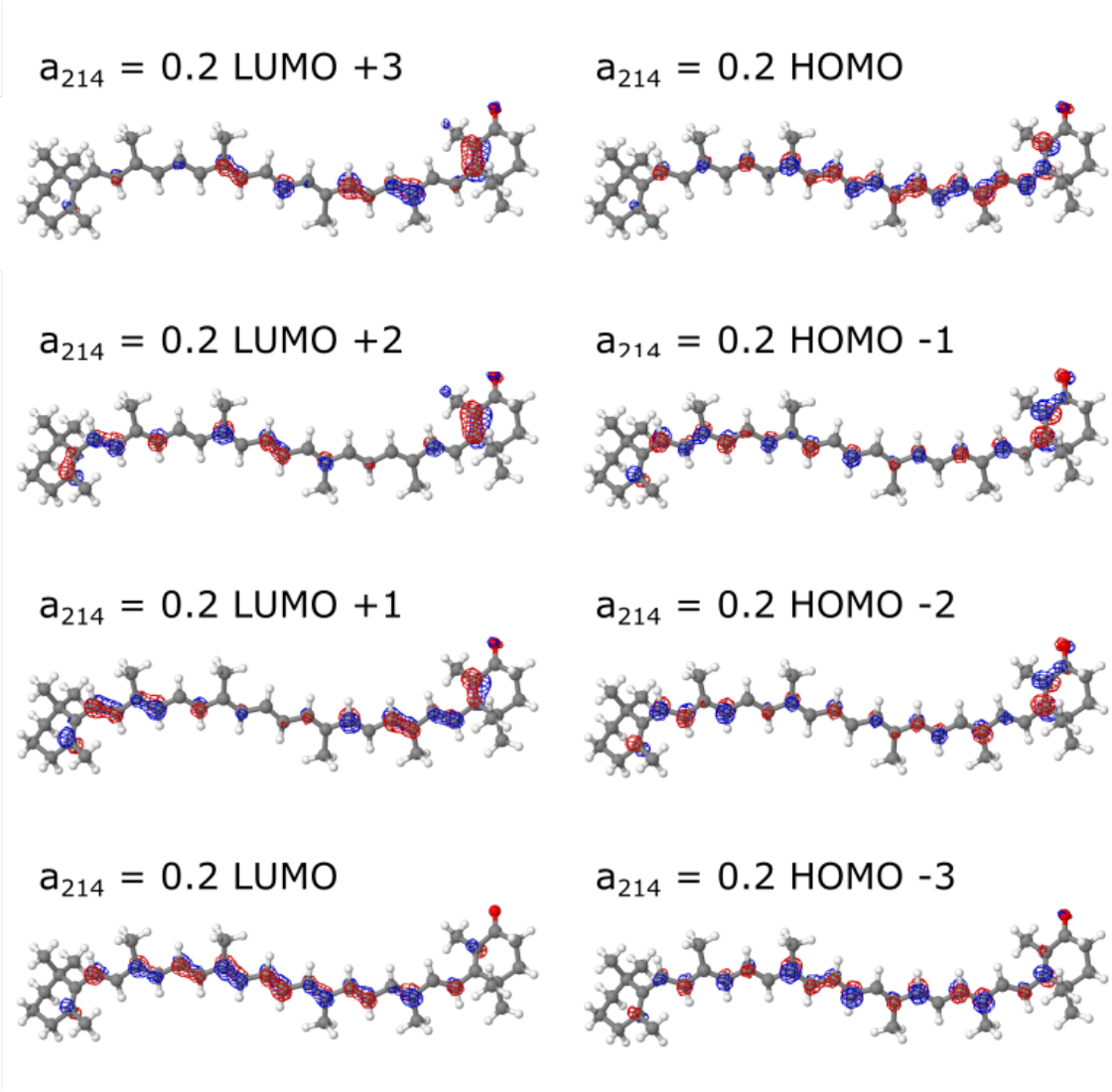

Fig. 3 Visualization the AM1-MECI active space calculated for a distortion along normal mode 214 (a C=C stretching mode) of amplitude $a_0 = 0.2$. There is no quantitative change with respect to the equilibrium geometry.

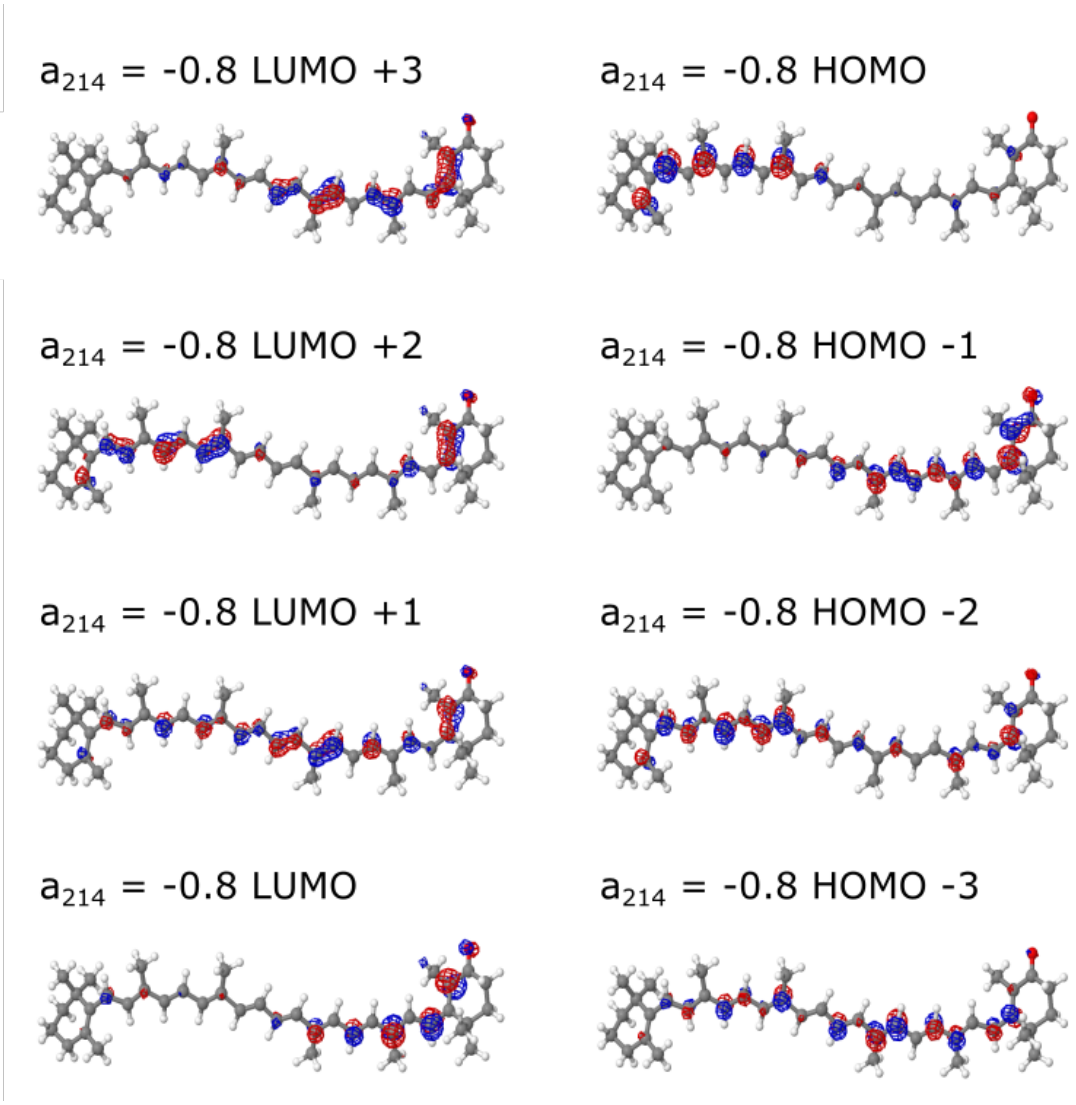

Fig. 4 Visualization the AM1-MECI active space calculated for a distortion along normal mode 214 of amplitude $a_214 = -0.8$. This represents a significant perturbation to the BLA and results in the HOMO and LUMO particularly becoming highly-distorted. The subsequent excited state calculations becoming unreliable. BLA distortions this severe are not sampled at room temperature.

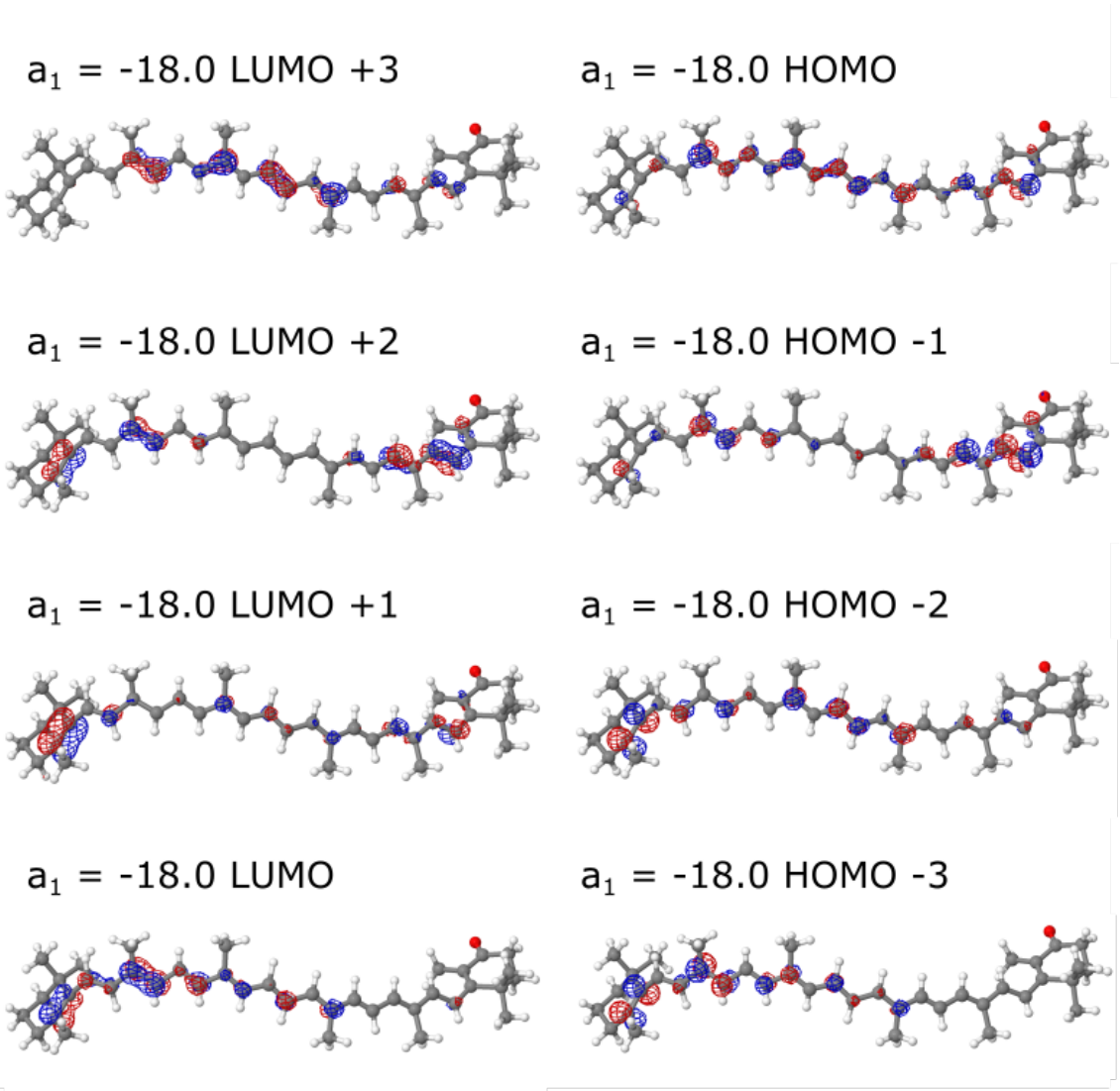

Fig. 5 Visualization of the AM1-MECI active space calculated for a very large distortion along normal mode 1 (low frequency bending) of amplitude $a_1 = -18$. This clearly results in some perturbation to orbitals, particularly a reduction in amplitude at centre of the chain (the site of the bend). This represents the typical distortion enforced by the the OCP$_o$ binding pocket. However, the perturbations to the frontier orbitals appear to be physically relevant as computation of the energies, TDM and spectra gives valid results despite the strong distortion.

2 Force Field Parameters for Echinenone

The custom atom types defined for Ech are shown in Supp. Fig. 1. For comparison the far more general GAFF atom types are also shown. All parameters are listed below in standard format.

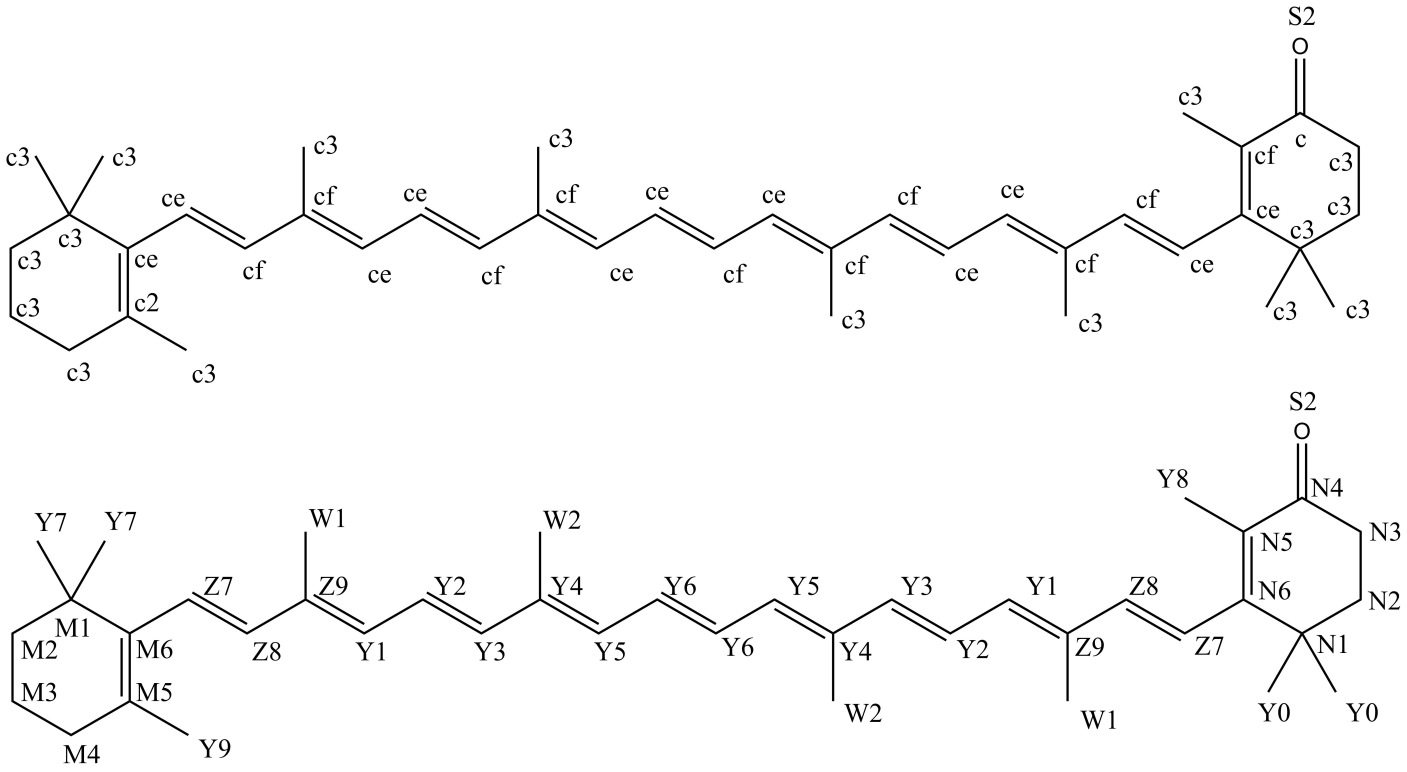

Fig. 6 Atom types for echinenone as defined within the GAFF (top) and the *ad hoc* FF (bottom).

ECH
MASS
M1 12.01 0.0
M2 12.01 0.0
M3 12.01 0.0
M4 12.01 0.0
M5 12.01 0.0
M6 12.01 0.0
N1 12.01 0.0
N2 12.01 0.0
N3 12.01 0.0
N4 12.01 0.0
N5 12.01 0.0
N6 12.01 0.0
Z7 12.01 0.0
Z8 12.01 0.0
Z9 12.01 0.0
Y1 12.01 0.0
Y2 12.01 0.0
Y3 12.01 0.0
Y4 12.01 0.0
Y5 12.01 0.0
Y6 12.01 0.0
Y7 12.01 0.0
Y8 12.01 0.0
Y9 12.01 0.0
Y0 12.01 0.0
W1 12.01 0.0
W2 12.01 0.0
S2 16.0 0.0
U2 1.008 0.0
U3 1.008 0.0
U5 1.008 0.0
U6 1.008 0.0
U7 1.008 0.0
U8 1.008 0.0
U9 1.008 0.0
T1 1.008 0.0
T2 1.008 0.0
T3 1.008 0.0
T4 1.008 0.0
T5 1.008 0.0
R1 1.008 0.0
R4 1.008 0.0
R5 1.008 0.0
R7 1.008 0.0
V1 1.008 0.0
V2 1.008 0.0

BOND
M1-M2 262.5788 1.5452

M1-M6 257.4902 1.5481
M1-Y7 259.66116 1.5495
M1-Y7 259.66116 1.5495
M2-M3 284.6635 1.5246
M2-U2 331.18668 1.0971
M2-U2 331.18668 1.0971
M3-M4 285.3356 1.5273
M3-U3 335.33082 1.0951
M3-U3 335.33082 1.0951
M4-M5 279.587 1.5160
M4-U5 332.51427 1.0960
M4-U5 332.51427 1.0960
M5-M6 567.4438 1.3539
M5-Y9 296.07237 1.5102
M6-Z7 258.4424 1.4742
Z7-Z8 444.1184 1.3546
Z7-U6 359.24427 1.0859
Z8-Z9 288.196 1.4513
Z8-U7 369.63828 1.0823
Z9-Y1 430.096 1.3671
Z9-W1 242.2912 1.5074
Y1-Y2 303.216 1.4321
Y1-U8 352.91718 1.0888
Y2-Y3 430.096 1.3671
Y2-U9 365.63076 1.0840
Y3-Y4 303.216 1.4321
Y3-T1 352.91718 1.0888
Y4-Y5 430.096 1.3671
Y4-W2 242.2912 1.5074
Y5-Y6 308.832 1.4266
Y5-T2 352.91718 1.0888
Y6-Y6 423.5776 1.3657
Y6-T3 359.72541 1.0861
Y6-Y5 308.832 1.4266
Y6-T3 359.72541 1.0861
Y5-Y4 430.096 1.3671
Y5-T2 352.91718 1.0888
Y4-Y3 303.216 1.4321
Y4-W2 242.2912 1.5074
Y3-Y2 430.096 1.3671
Y3-T1 352.91718 1.0888
Y2-Y1 303.216 1.4321
Y2-U9 365.63076 1.0840
Y1-Z9 430.096 1.3671
Y1-U8 352.91718 1.0888
Z9-Z8 288.196 1.4513
Z9-W1 299.83536 1.5074
Z8-Z7 444.1184 1.3546
Z8-U7 369.63828 1.0823
Z7-N6 262.8792 1.4724
Z7-U6 359.24427 1.0859

N6-N5 523.6484 1.3686
N6-N1 262.317 1.5436
N5-N4 296.7283 1.4857
N5-Y8 299.18988 1.5108
N4-S2 808.592 1.2207
N4-N3 273.8945 1.5137
N3-N2 287.7028 1.5226
N3-V1 344.46456 1.0920
N3-V1 344.46456 1.0920
N2-N1 263.3092 1.5447
N2-V2 333.21816 1.0963
N2-V2 333.21816 1.0963
N1-Y0 259.66116 1.5495
N1-Y0 259.66116 1.5495
Y7-T4 345.51396 1.0920
Y7-T4 345.51396 1.0920
Y7-T4 345.51396 1.0920
Y7-T4 345.51396 1.0920
Y7-T4 345.51396 1.0920
Y7-T4 345.51396 1.0920
Y9-R1 354.55563 1.0882
Y9-R1 354.55563 1.0882
Y9-R1 354.55563 1.0882
W1-R4 337.92264 1.0951
W1-R4 337.92264 1.0951
W1-R4 337.92264 1.0951
W2-R7 337.92264 1.0951
W2-R7 337.92264 1.0951
W2-R7 337.92264 1.0951
W2-R7 337.92264 1.0951
W2-R7 337.92264 1.0951
W2-R7 337.92264 1.0951
W1-R4 337.92264 1.0951
W1-R4 337.92264 1.0951
W1-R4 337.92264 1.0951
Y8-R5 353.78739 1.0890
Y8-R5 353.78739 1.0890
Y8-R5 353.78739 1.0890
Y0-T5 345.51396 1.0920
Y0-T5 345.51396 1.0920
Y0-T5 345.51396 1.0920
Y0-T5 345.51396 1.0920
Y0-T5 345.51396 1.0920
Y0-T5 345.51396 1.0920

ANGLE
M1-M2-M3 70.8400 112.9200
M1-M2-U2 45.9225 108.6800
M1-M2-U2 45.9225 108.6800
M1-M6-M5 94.0400 122.5300
M1-M6-Z7 52.2190 114.2000

M1-Y7-T4 41.8320 111.9900
M1-Y7-T4 41.8320 111.9900
M1-Y7-T4 41.8320 111.9900
M1-Y7-T4 41.8320 111.9900
M1-Y7-T4 41.8320 111.9900
M1-Y7-T4 41.8320 111.9900
M2-M1-M6 39.7300 110.9300
M2-M1-Y7 51.1600 107.3700
M2-M1-Y7 51.1600 107.3700
M2-M3-M4 80.9450 109.7200
M2-M3-U3 42.5700 110.1800
M2-M3-U3 42.5700 110.1800
M3-M2-U2 44.0595 108.7100
M3-M2-U2 44.0595 108.7100
M3-M4-M5 95.6750 114.2300
M3-M4-U5 62.5815 110.1800
M3-M4-U5 62.5815 110.1800
M4-M3-U3 41.4045 109.6100
M4-M3-U3 41.4045 109.6100
M4-M5-M6 115.1800 122.6800
M4-M5-Y9 232.8300 112.8700
M5-M4-U5 55.3095 108.8900
M5-M4-U5 55.3095 108.8900
M5-M6-Z7 51.3280 123.2200
M5-Y9-R1 41.5464 113.0800
M5-Y9-R1 41.5464 113.0800
M5-Y9-R1 41.5464 113.0800
M6-M1-Y7 42.0750 110.4700
M6-M1-Y7 42.0750 110.4700
M6-M5-Y9 234.4950 124.4500
M6-Z7-Z8 33.8120 126.9300
M6-Z7-U6 27.0910 115.2200
Z7-Z8-Z9 44.9040 125.3700
Z7-Z8-U7 29.8810 119.8800
Z8-Z7-U6 31.5130 116.3600
Z8-Z9-Y1 52.7840 117.8900
Z8-Z9-W1 52.9010 118.8600
Z9-Z8-U7 30.3710 114.7000
Z9-Y1-Y2 44.9940 128.2000
Z9-Y1-U8 31.1340 116.6000
Z9-W1-R4 40.4754 110.8700
Z9-W1-R4 40.4754 110.8700
Z9-W1-R4 40.4754 110.8700
Y1-Z9-W1 54.2110 123.2500
Y1-Y2-Y3 36.0950 122.9400
Y1-Y2-U9 27.3690 118.2500
Y2-Y1-U8 30.3950 115.2100
Y2-Y3-Y4 44.9940 128.2000
Y2-Y3-T1 30.3950 115.2100
Y3-Y2-U9 27.3690 118.2500
Y3-Y4-Y5 51.3330 118.2600

Y3-Y4-W2 54.2110 123.2500
Y4-Y3-T1 31.1340 116.6000
Y4-Y5-Y6 44.7470 128.2000
Y4-Y5-T2 31.1340 116.6000
Y4-W2-R7 40.4754 110.8700
Y4-W2-R7 40.4754 110.8700
Y4-W2-R7 40.4754 110.8700
Y5-Y4-W2 54.2110 123.2500
Y5-Y6-Y6 35.5960 123.5400
Y5-Y6-T3 27.1700 118.7500
Y6-Y5-T2 30.2770 115.3300
Y6-Y6-Y5 35.5960 123.5400
Y6-Y6-T3 27.4390 117.7100
Y6-Y6-T3 27.4390 117.7100
Y6-Y5-Y4 44.7470 128.2000
Y6-Y5-T2 30.2770 115.3300
Y5-Y6-T3 27.1700 118.7500
Y5-Y4-Y3 51.3330 118.2600
Y5-Y4-W2 54.2110 123.2500
Y4-Y5-T2 31.1340 116.6000
Y4-Y3-Y2 44.9940 128.2000
Y4-Y3-T1 31.1340 116.6000
Y4-W2-R7 40.4754 110.8700
Y4-W2-R7 40.4754 110.8700
Y4-W2-R7 40.4754 110.8700
Y3-Y4-W2 54.2110 123.2500
Y3-Y2-Y1 36.0950 122.9400
Y3-Y2-U9 27.3690 118.2500
Y2-Y3-T1 30.3950 115.2100
Y2-Y1-Z9 44.9940 128.2000
Y2-Y1-U8 30.3950 115.2100
Y1-Y2-U9 27.3690 118.2500
Y1-Z9-Z8 52.7840 117.8900
Y1-Z9-W1 54.2110 123.2500
Z9-Y1-U8 31.1340 116.6000
Z9-Z8-Z7 44.9040 125.3700
Z9-Z8-U7 30.3710 114.7000
Z9-W1-R4 40.4754 110.8700
Z9-W1-R4 40.4754 110.8700
Z9-W1-R4 40.4754 110.8700
Z8-Z9-W1 52.9010 118.8600
Z8-Z7-U6 31.5130 116.3600
Z7-Z8-U7 29.8810 119.8800
Z7-N6-N5 57.6850 116.4900
Z7-N6-N1 61.7760 121.1100
N6-Z7-U6 30.9130 113.2300
N6-Z7-Z8 44.6350 130.3000
N6-N5-N4 124.9000 122.6400
N6-N5-Y8 235.4450 122.6300
N6-N1-N2 40.2600 110.1800
N6-N1-Y0 37.8300 107.8500

N6-N1-Y0 37.8300 107.8500
N5-N6-N1 97.7150 121.9800
N5-N4-S2 85.0500 121.7100
N5-N4-N3 105.9700 117.5100
N5-Y8-R5 44.2134 109.1300
N5-Y8-R5 44.2134 109.1300
N5-Y8-R5 44.2134 109.1300
N4-N5-Y8 252.3500 114.7100
N4-N3-N2 87.3650 111.5400
N4-N3-V1 51.6330 107.9200
N4-N3-V1 51.6330 107.9200
S2-N4-N3 82.5642 120.7500
N3-N2-N1 74.1100 113.5700
N3-N2-V2 44.8740 108.8300
N3-N2-V2 44.8740 108.8300
N2-N3-V1 55.2285 112.2200
N2-N3-V1 55.2285 112.2200
N2-N1-Y0 43.3900 110.5100
N2-N1-Y0 43.3900 110.5100
N1-N2-V2 46.5660 108.3300
N1-N2-V2 46.5660 108.3300
N1-Y0-T5 41.8320 111.9900
N1-Y0-T5 41.8320 111.9900
N1-Y0-T5 41.8320 111.9900
N1-Y0-T5 41.8320 111.9900
N1-Y0-T5 41.8320 111.9900
Y7-M1-Y7 51.4950 107.7700
Y0-N1-Y0 51.4950 107.7700
U2-M2-U2 33.5120 106.5100
U3-M3-U3 35.4640 106.4800
U5-M4-U5 42.5760 105.1800
V1-N3-V1 43.4400 106.5600
V2-N2-V2 33.5600 106.5700
T4-Y7-T4 32.9824 107.6800
T4-Y7-T4 32.9824 107.6800
T4-Y7-T4 32.9824 107.6800
T4-Y7-T4 32.9824 107.6800
T4-Y7-T4 32.9824 107.6800
T4-Y7-T4 32.9824 107.6800
R1-Y9-R1 35.5938 107.8200
R1-Y9-R1 35.5938 107.8200
R1-Y9-R1 35.5938 107.8200
R4-W1-R4 34.8502 106.9900
R4-W1-R4 34.8502 106.9900
R4-W1-R4 34.8502 106.9900
R7-W2-R7 34.8502 106.9900
R7-W2-R7 34.8502 106.9900
R7-W2-R7 34.8502 106.9900
R7-W2-R7 34.8502 106.9900
R7-W2-R7 34.8502 106.9900
R7-W2-R7 34.8502 106.9900

R4-W1-R4 34.8502 106.9900
R4-W1-R4 34.8502 106.9900
R4-W1-R4 34.8502 106.9900
R5-Y8-R5 35.1164 107.1300
R5-Y8-R5 35.1164 107.1300
R5-Y8-R5 35.1164 107.1300
T5-Y0-T5 32.9824 107.6800
T5-Y0-T5 32.9824 107.6800
T5-Y0-T5 32.9824 107.6800
T5-Y0-T5 32.9824 107.6800
T5-Y0-T5 32.9824 107.6800
T5-Y0-T5 32.9824 107.6800

DIHE
M1-M2-M3-M4 1.0000 0.1800 0.0000 -3.0000
M1-M2-M3-M4 1.0000 0.2500 180.0000 -2.0000
M1-M2-M3-M4 1.0000 0.2000 180.0000 1.0000
M1-M2-M3-U3 1.0000 0.1600 0.0000 3.0000
M1-M6-M5-Y9 6.0000 0.0000 0.0000 2.0000
M1-M6-Z7-Z8 1.0000 4.0000 180.0000 2.0000
M1-M6-Z7-U6 1.0000 4.0000 180.0000 2.0000
M2-M3-M4-M5 1.0000 0.1560 0.0000 3.0000
M2-M3-M4-U5 1.0000 0.1600 0.0000 3.0000
M2-M1-Y7-T4 1.0000 0.1600 0.0000 3.0000
M2-M1-M6-M5 1.0000 0.0000 0.0000 2.0000
M2-M1-M6-Z7 1.0000 0.0000 0.0000 2.0000
M3-M4-M5-Y9 1.0000 0.0000 0.0000 2.0000
M3-M4-M5-M6 1.0000 0.0000 0.0000 2.0000
M3-M2-M1-Y7 1.0000 0.1800 0.0000 -3.0000
M3-M2-M1-Y7 1.0000 0.2500 180.0000 -2.0000
M3-M2-M1-Y7 1.0000 0.2000 180.0000 1.0000
M3-M2-M1-M6 1.0000 0.1560 0.0000 3.0000
M4-M5-M6-M1 1.0000 6.5000 180.0000 2.0000
M4-M5-M6-Z7 1.0000 6.5000 180.0000 2.0000
M4-M5-Y9-R1 1.0000 0.0000 0.0000 2.0000
M4-M3-M2-U2 1.0000 0.1600 0.0000 3.0000
M5-M6-M1-Y7 1.0000 0.0000 0.0000 2.0000
M5-M6-Z7-Z8 1.0000 4.0000 180.0000 2.0000
M5-M6-Z7-U6 1.0000 1.0000 180.0000 2.0000
M5-M4-M3-U3 1.0000 0.1600 0.0000 3.0000
M6-M1-M2-U2 1.0000 0.1560 0.0000 3.0000
M6-M1-Y7-T4 1.0000 0.1600 0.0000 3.0000
M6-M5-Y9-R1 1.0000 0.0000 0.0000 2.0000
M6-M5-M4-U5 1.0000 0.0000 0.0000 2.0000
M6-Z7-Z8-Z9 1.0000 16.500 180.0000 -2.0000
M6-Z7-Z8-Z9 1.0000 10.650 357.5000 2.0000
M6-Z7-Z8-U7 1.0000 8.5900 180.0000 2.0000
Y7-M1-M2-U2 1.0000 0.1600 0.0000 3.0000
Y7-M1-M6-Z7 1.0000 7.5000 180.0000 2.0000
Y7-M1-Y7-T4 1.0000 0.1600 0.0000 3.0000
U2-M2-M3-U3 1.0000 0.1500 0.0000 3.0000

U3-M3-M4-U5 1.0000 0.1500 0.0000 3.0000
U5-M4-M5-Y9 1.0000 0.0000 0.0000 2.0000
Y9-M5-M6-Z7 1.0000 7.5000 180.0000 2.0000
Z7-Z8-Z9-Y1 1.0000 4.0000 180.0000 2.0000
Z7-Z8-Z9-W1 1.0000 4.0000 180.0000 2.0000
Z8-Z9-Y1-Y2 1.0000 4.0000 180.0000 2.0000
Z8-Z9-Y1-U8 1.0000 4.0000 180.0000 2.0000
Z8-Z9-W1-R4 1.0000 0.0000 0.0000 2.0000
Z9-Y1-Y2-Y3 1.0000 4.0000 180.0000 2.0000
Z9-Y1-Y2-U9 1.0000 4.0000 180.0000 2.0000
R4-W1-Z9-Y1 1.0000 0.0000 0.0000 2.0000
W1-Z9-Y1-Y2 1.0000 4.0000 180.0000 2.0000
W1-Z9-Y1-U8 1.0000 4.0000 180.0000 2.0000
Y1-Y2-Y3-Y4 1.0000 4.0000 180.0000 2.0000
Y1-Y2-Y3-T1 1.0000 4.0000 180.0000 2.0000
Y2-Y3-Y4-Y5 1.0000 4.0000 180.0000 2.0000
Y2-Y3-Y4-W2 1.0000 4.0000 180.0000 2.0000
Y3-Y4-Y5-Y6 1.0000 4.0000 180.0000 2.0000
Y3-Y4-Y5-T2 1.0000 4.0000 180.0000 2.0000
Y3-Y4-W2-R7 1.0000 0.0000 0.0000 2.0000
Y4-Y5-Y6-Y6 1.0000 4.0000 180.0000 2.0000
Y4-Y5-Y6-T3 1.0000 4.0000 180.0000 2.0000
Y5-Y6-Y6-Y5 1.0000 4.0000 180.0000 2.0000
Y5-Y6-Y6-T3 1.0000 4.0000 180.0000 2.0000
Y6-Y6-Y5-T2 1.0000 4.0000 180.0000 2.0000
U6-Z7-Z8-Z9 1.0000 4.0000 180.0000 2.0000
U6-Z7-Z8-U7 1.0000 6.6500 180.0000 2.0000
U7-Z8-Z9-Y1 1.0000 4.0000 180.0000 2.0000
U7-Z8-Z9-W1 1.0000 4.0000 180.0000 2.0000
U8-Y1-Y2-Y3 1.0000 4.0000 180.0000 2.0000
U8-Y1-Y2-U9 1.0000 4.0000 180.0000 2.0000
U9-Y2-Y3-Y4 1.0000 4.0000 180.0000 2.0000
U9-Y2-Y3-T1 1.0000 4.0000 180.0000 2.0000
T1-Y3-Y4-W2 1.0000 4.0000 180.0000 2.0000
T1-Y3-Y4-Y5 1.0000 4.0000 180.0000 2.0000
R7-W2-Y4-Y5 1.0000 0.0000 0.0000 2.0000
W2-Y4-Y5-Y6 1.0000 4.0000 180.0000 2.0000
W2-Y4-Y5-T2 1.0000 4.0000 180.0000 2.0000
T2-Y5-Y6-T3 1.0000 4.0000 180.0000 2.0000
T3-Y6-Y6-T3 1.0000 4.0000 180.0000 2.0000
N1-N2-N3-N4 1.0000 0.2000 180.0000 1.0000
N1-N2-N3-V1 1.0000 0.1600 0.0000 3.0000
N2-N3-N4-N5 1.0000 0.1560 0.0000 3.0000
N2-N3-N4-S2 1.0000 0.7400 0.0000 1.0000
N3-N4-N5-N6 1.0000 8.7000 0.0000 2.0000
N3-N4-N5-Y8 1.0000 0.0000 0.0000 2.0000
N4-N5-N6-N1 1.0000 6.6500 180.0000 2.0000
N4-N5-N6-Z7 1.0000 6.6500 180.0000 2.0000
N4-N5-Y8-R5 1.0000 0.0000 0.0000 2.0000
N5-N6-N1-N2 1.0000 0.0000 0.0000 2.0000
N5-N6-N1-Y0 1.0000 0.0000 0.0000 2.0000

N5-N6-Z7-Z8 1.0000 4.0000 180.0000 2.0000
N5-N6-Z7-U6 1.0000 4.0000 180.0000 2.0000
N6-N1-N2-N3 1.0000 0.1560 0.0000 3.0000
N6-N1-N2-V2 1.0000 0.1560 0.0000 3.0000
N6-N1-Y0-T5 1.0000 0.1600 0.0000 3.0000
T5-Y0-N1-N2 1.0000 0.1600 0.0000 3.0000
T5-Y0-N1-Y0 1.0000 0.1600 0.0000 3.0000
Y0-N1-N2-N3 1.0000 0.2000 180.0000 1.0000
Y0-N1-N2-V2 1.0000 0.1600 0.0000 3.0000
V2-N2-N3-N4 1.0000 0.1600 0.0000 3.0000
V2-N2-N3-V1 1.0000 0.1500 0.0000 3.0000
V1-N3-N4-N5 1.0000 0.1500 0.0000 3.0000
V1-N3-N4-S2 1.0000 0.0400 29.8000 3.0000
S2-N4-N5-Y8 4.0000 8.7000 180.0000 2.0000
S2-N4-N5-N6 4.0000 8.7000 180.0000 2.0000
R5-Y8-N5-N6 1.0000 0.0000 0.0000 2.0000
Y8-N5-N6-N1 6.0000 6.6500 0.0000 2.0000
Y8-N5-N6-Z7 1.0000 6.6500 180.0000 2.0000
Z7-N6-N1-N2 1.0000 0.0000 0.0000 2.0000
Z7-N6-N1-Y0 1.0000 7.5000 180.0000 2.0000
Z8-Z7-N6-N1 1.0000 4.0000 180.0000 2.0000
Z9-Z8-Z7-N6 1.0000 4.0000 180.0000 2.0000
U6-Z7-N6-N1 1.0000 4.0000 180.0000 2.0000
U7-Z8-Z7-N6 1.0000 8.5900 180.0000 2.0000

NONBON
M1 1.908 0.086
M2 1.908 0.086
M3 1.908 0.086
M4 1.908 0.086
M5 1.908 0.086
M6 1.908 0.086
N1 1.908 0.086
N2 1.908 0.086
N3 1.908 0.086
N4 1.908 0.086
N5 1.908 0.086
N6 1.908 0.086
Z7 1.908 0.086
Z8 1.908 0.086
Z9 1.908 0.086
Y1 1.908 0.086
Y2 1.908 0.086
Y3 1.908 0.086
Y4 1.908 0.086
Y5 1.908 0.086
Y6 1.908 0.086
Y7 1.908 0.086
Y8 1.908 0.086
Y9 1.908 0.086
Y0 1.908 0.086

W1 1.908 0.086
W2 1.908 0.086
S2 1.721 0.2104
U2 1.487 0.0157
U3 1.3870 0.0157
U5 1.487 0.0157
U6 1.4590 0.0150
U7 1.4590 0.0150
U8 1.4590 0.0150
U9 1.4590 0.0150
T1 1.4590 0.0150
T2 1.4590 0.0150
T3 1.4590 0.0150
T4 1.487 0.0157
T5 1.487 0.0157
R1 1.487 0.0157
R4 1.487 0.0157
R5 1.487 0.0157
R7 1.487 0.0157
V1 1.487 0.0157
V2 1.487 0.0157

GOL parameters

5TUX_GOL
MASS
c3 12.010 0.878
oh 16.000 0.465
ho 1.008 0.135
h1 1.008 0.135

BOND
c3-oh 293.40 1.423
c3-c3 232.52 1.538
c3-h1 375.92 1.097
ho-oh 563.51 0.973

ANGLE
c3-oh-ho 49.027 107.260
c3-c3-oh 84.642 110.190
c3-c3-c3 64.888 111.510
c3-c3-h1 46.868 109.560
h1-c3-oh 62.540 110.260
h1-c3-h1 38.802 108.460

DIHE
c3-c3-oh-ho 1 0.000 0.000 3.000
c3-c3-c3-oh 1 0.210 0.000 3.000
c3-c3-c3-h1 9 1.400 0.000 3.000
oh-c3-c3-oh 1 0.900 0.000 -3.000
oh-c3-c3-oh 1 1.130 0.000 2.000
h1-c3-c3-oh 1 0.000 0.000 -3.000

h1-c3-c3-oh 1 0.250 0.000 1.000
h1-c3-oh-ho 1 0.113 0.000 3.000
h1-c3-c3-h1 9 1.400 0.000 3.000

IMPROPER

NONBON
c3 1.9069 0.1078
oh 1.8200 0.0930
ho 0.3019 0.0047
h1 1.3593 0.0208

3 Echinenone Force Field Validation

3.1 Structural properties

Supp. Fig. 7 compares BLA as calculated quantum chemically and using our finely tuned FF. The 'DFT' values represent the equilibrium bond lengths as produced by a B3LYP/6-311G(d,p) optimization in vacuo. The 'MD' values are averages over short in vacuo MD runs. As with previous work on related carotenoids[1] the agreement is very good but for a slight systematic over-estimate. This is due to the inherent inaccuracy in representing a delocalized system as a chain of localized, pair-wise interactions. This FF is an enormous improvement on the GAFF which assumes a far more uniform BLA along the conjugated chain.

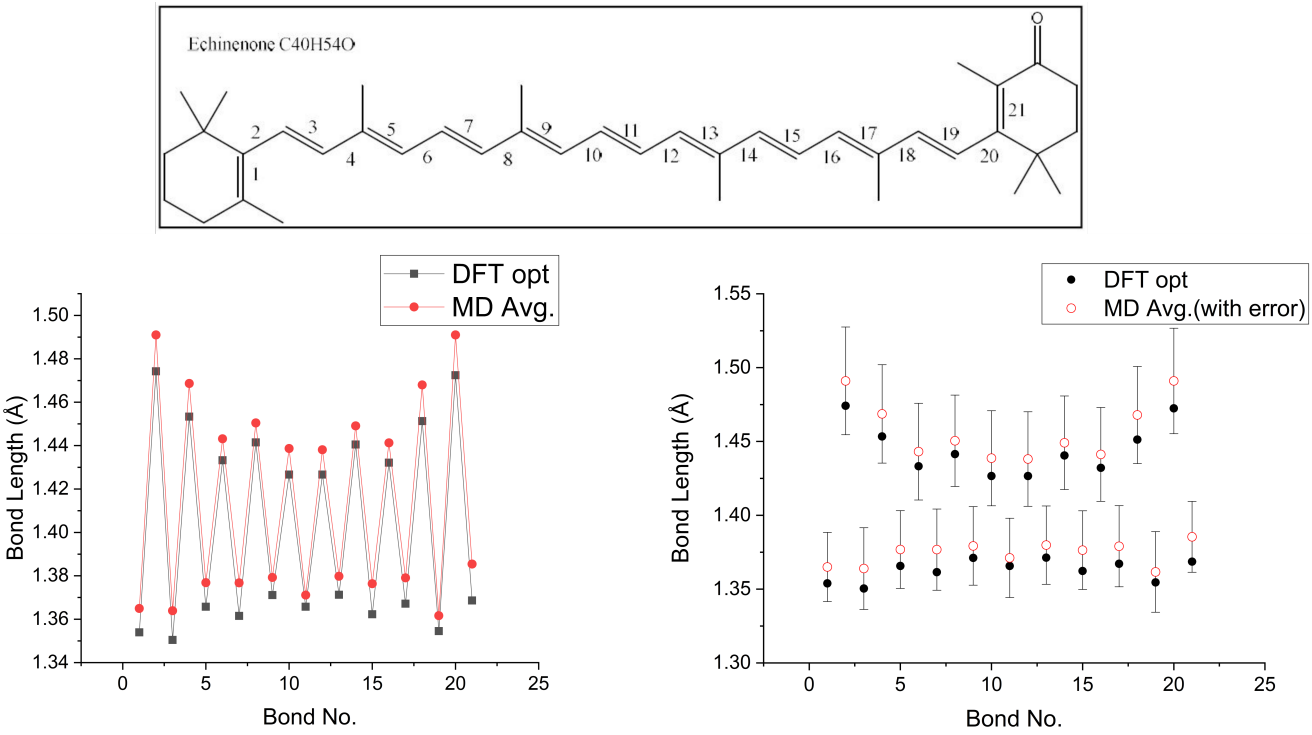

Fig. 7 The bond lengths of the C-C and C=C bonds along the echinenone conjugated backbone. The numerical labelling is indicated by the structural formula of *cis-cis* Ech. **Bottom left:** Comparison of the *in vacuo* equilibrium bond lengths as calculated by B3LYP/6-311G(d,p) ("DFT opt") with the average bond lengths calculated from a short equilibrium MD run ("MD Avg."). **Bottom right:** The same bond lengths plus the standard deviations of the MD values shown as error bars.

3.2 Vibrational properties

Supp. Fig. 8 compares the quantum chemical and classical FF vibrational normal modes of Ech *in vacuo*. The histogram in the left panel shows that we have excellent agreement between the quantum chemical and classical vibrations, particularly in the region of the optically active C-C (1100 $cm^{-}1$) and C=C (1500 $cm^{-}1$) modes. The only region where there is significant disagreement is in the high frequency hydrogen modes that are effectively irrelevant to this work. The right panel plots frequency against normal mode number for both cases and highlights the close agreement. Small differences in frequency are exaggerated in the histogram by the large bin width (100 $cm^{-}1$).

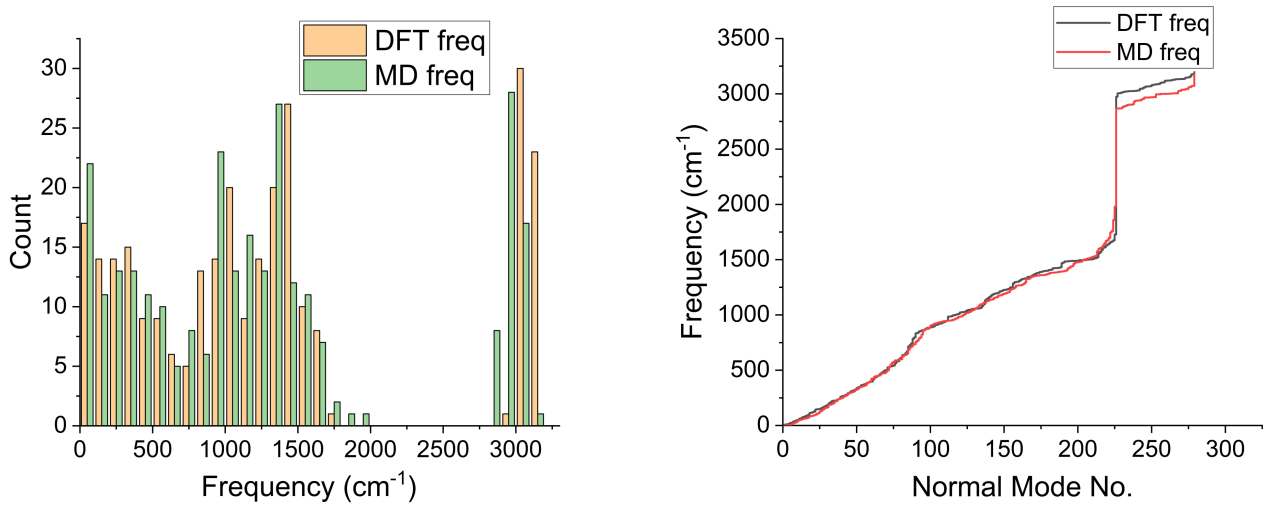

Fig. 8 Left: A histogram of Ech vibrational frequencies as calculated quantum chemically and classically using our finely tuned force field. A bin width of 100 $cm^{-}1$ is used. **Right:** A plot of quantum chemical and classical vibrational frequencies against normal mode number (ordered low frequency to high).

3.3 Excited state properties

Supp. Fig. 9 compares fluctuating excited state properties with the single point values calculated for the equilibrium B3LYP/6-311G(d,p) structure. Supp. Fig. 9 **A** shows the S_2 energy and indicates a slight over-estimate for the classical geometry relative to the quantum chemical one. **B** indicates much better agreement for the S_1 energy which is unsurprising since the AM1-MECI-OPEN(8,8) method was selected for its chemically relevant description of this state. **C** compares the DFT and MD TDMs indicating good agreement for S_1 and a slight systematic over-estimate for S_2.

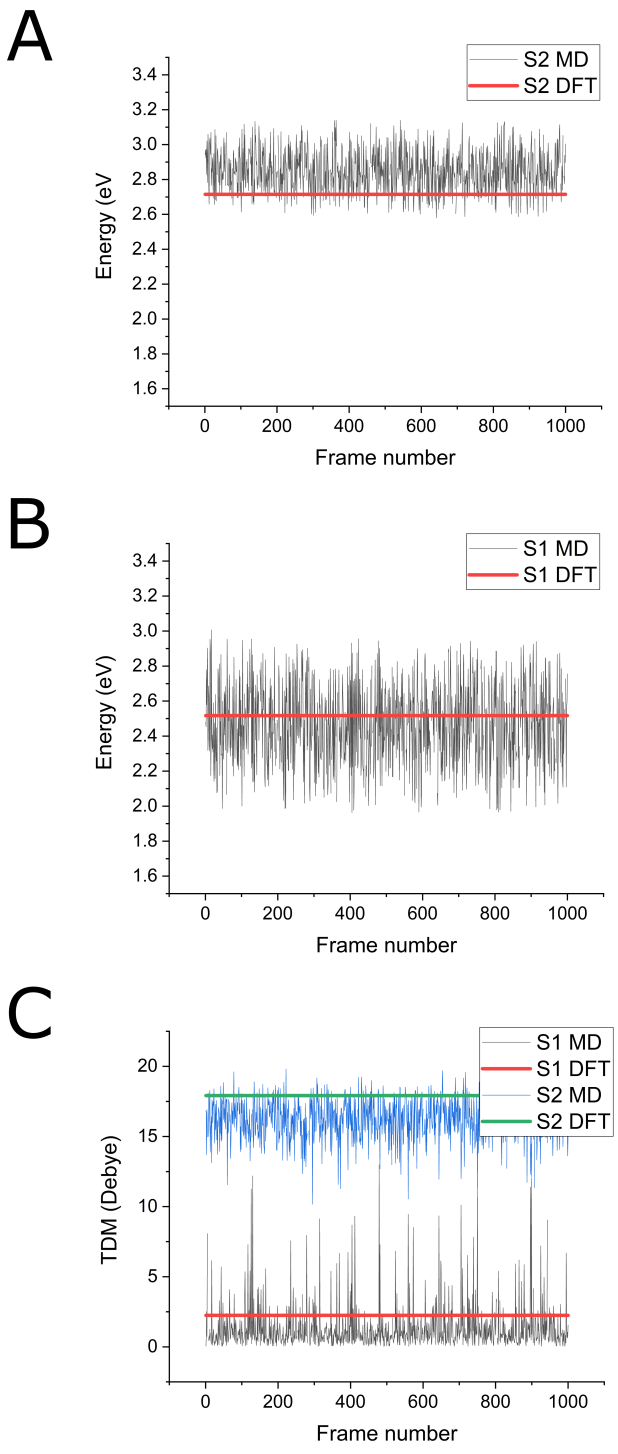

Fig. 9 A. S_2 vertical transition energies of MD snapshots (shown in black) and the B3LYP/6-311G(d,p) optimized structure (thick red line). **B.** S_1 vertical transition energies of MD snapshots (shown in black) and the DFT optimized structure (thick red line). **C.** The TDM of the S_1 and S_2 transitions for the MD snapshots and the B3LYP/6-311G(d,p) structure.

4 Visualization of the Normal Decomposition of Echinenone Structural Snapshots

In Supp. Fig. 10 we illustrate the two-step process of normal mode decomposition of a random structural snapshot of Ech. Supp. Fig. 10 **A** shows the initial rigid-body rotation and and centre-of-mass alignment of the snapshot (green) with the references structure (blue). Supp. Fig. 7 **B** includes the fit structure defined as a linear super-positions of normal distortions. The slight error comes from the exclusion of further refinement of the orientation during the fit. The splitting of the process in this way is used to ensure rapid convergence without the need for a carefully selected initial guess.

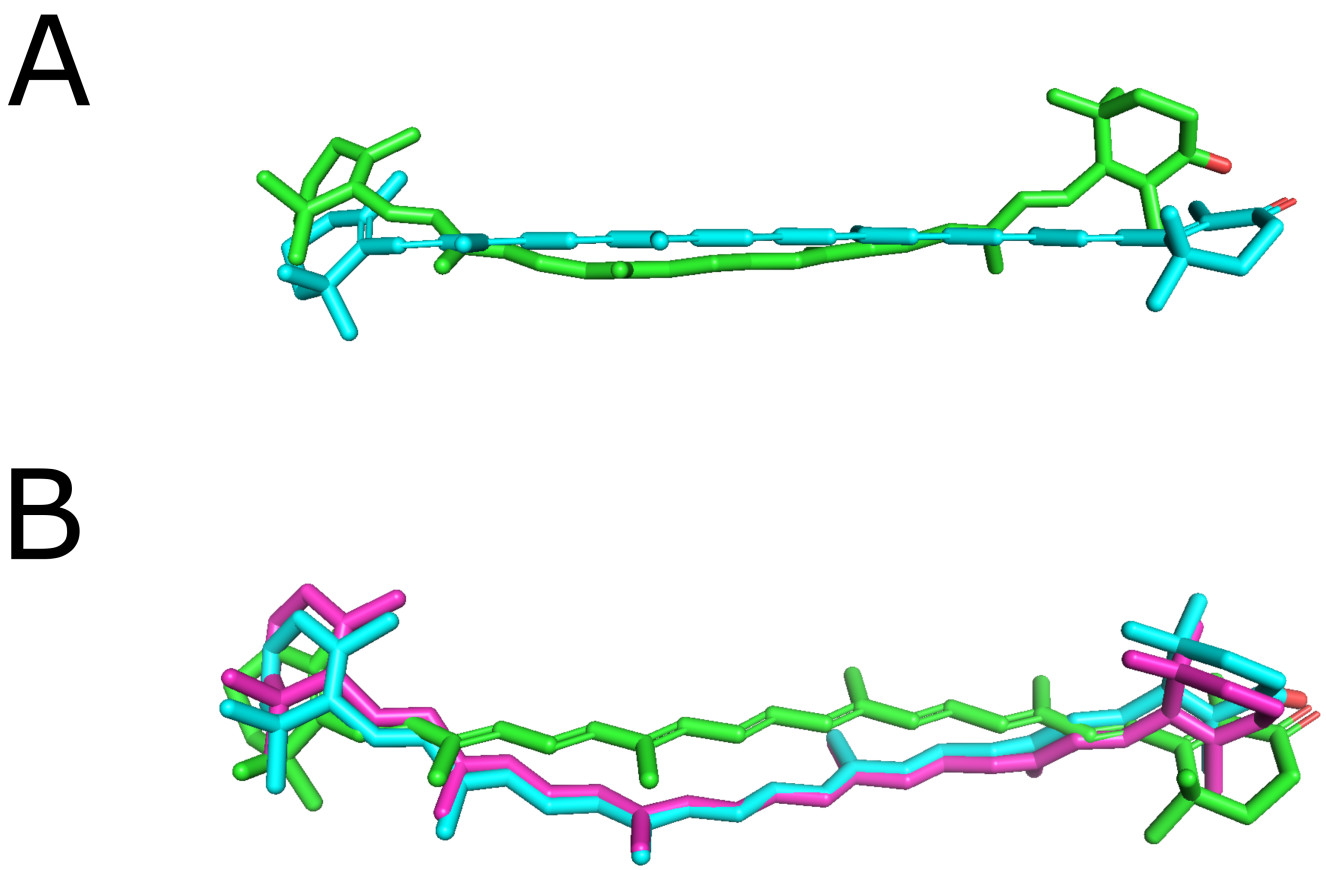

Fig. 10 A. The DFT-optimized (B3LYP/6-311G(d,p)) structure of echinenone (green) is used as a reference structure for fitting. The particular equilibrium structure is chosen depending on specific fit requirements with the *cis-cis* global minimum used for fitting Ech in THF and the *cis-trans* local minimum used for OCP_o. In the first step of the fitting the MD snapshot (blue) is rotated and translated to minimize the RMS deviations of the conjugated backbone carbons from the reference structure. **B.** The structure of a MD snapshot is reconstructed (magenta) by applying a linear combination of normal distortions to the reference structure.

5 Additional 2D Dihedral Scans

In Fig. 1 **D** and **E** of the main article we showed the 2D ground state potential energy surface for end-ring orientations and the S_1-S_2 energy gap. For completeness in Supp. Fig. 10 we show the absolute S_1 transition energy (**A**), the S_2 transition energy (**B**), the S_1 TDM, and the S_2 TDM across the same surface. As before the global minimum (magenta ring), local *cis-trans* minimum (red circle) and approximate position of Ech in OCP_o (black circle) are indicated. The TDM surfaces mirror the energy gap surface illustrating the basic principle that the S_1 optical properties are defined by state mixing. Although strong variations in optical properties can *in principle* be induced by end-ring rotations, the largest effects occur very far from low-energy structures.

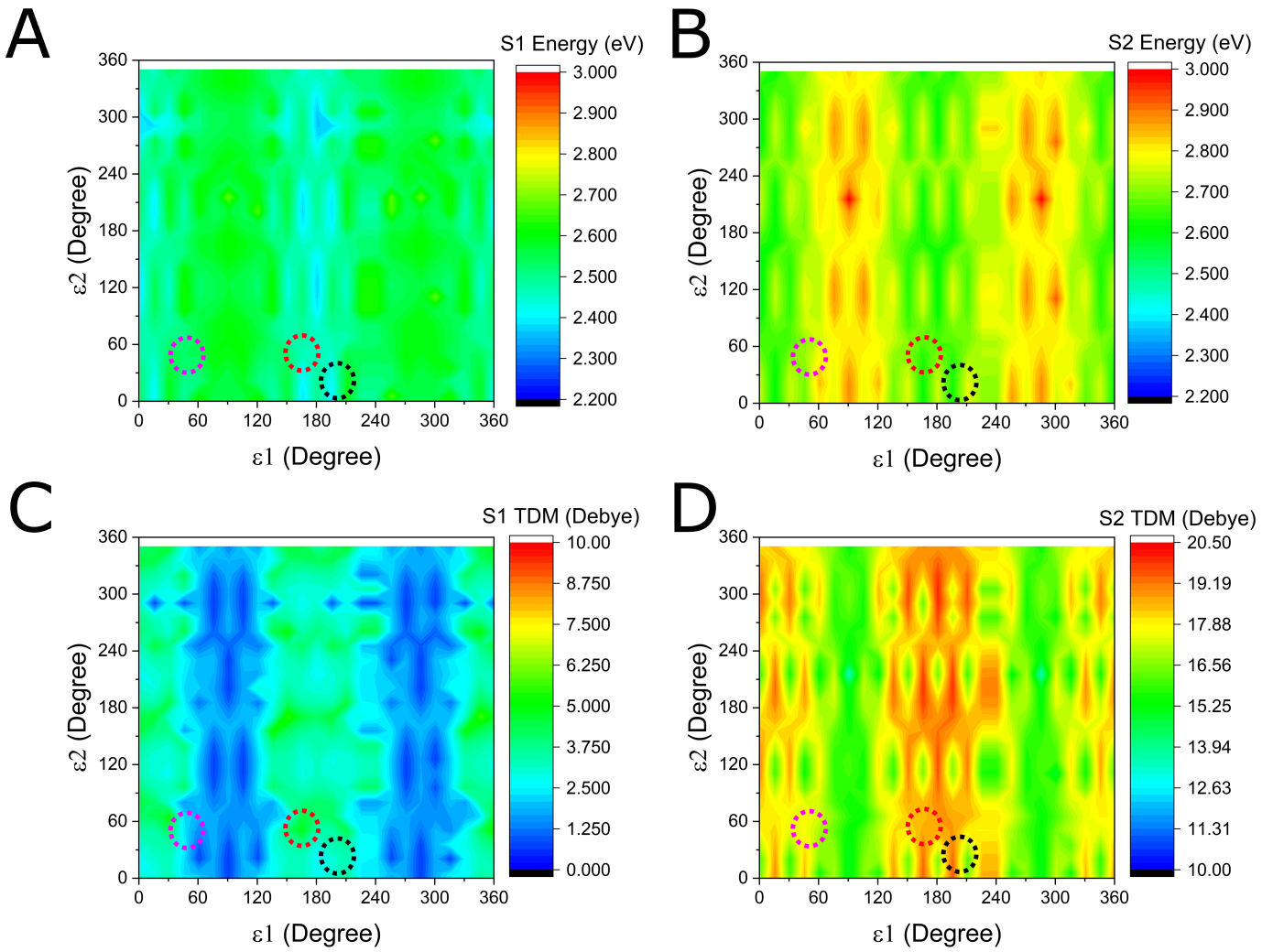

Fig. 11 A. S_0-S_1 transition energy surface as a function of end-ring rotations. **B.** S_0-S_2 transition energy surface as a function of end-ring rotations. **C.** S_1 transition dipole moment surface. Note the pattern mirrors that of the the S_1-S_2 energy gap surface shown in Fig. 1 **E** of the main article). **D.** S_2 transition dipole moment surface.

6 Normal Distortions and S_1-S_2 mixing

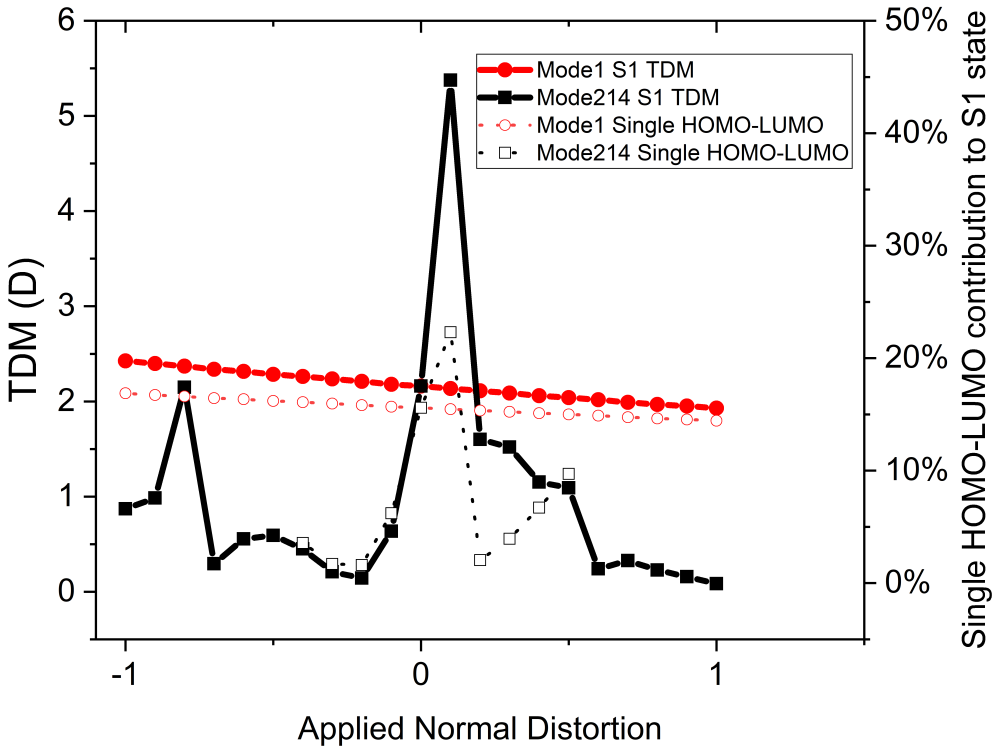

Fig. 12 Normal Mode scan on mode 1 and mode 214, with a double y axis showing the S1 TDM change and the S_1-S_2 Energy Gap along applied normal distortion.

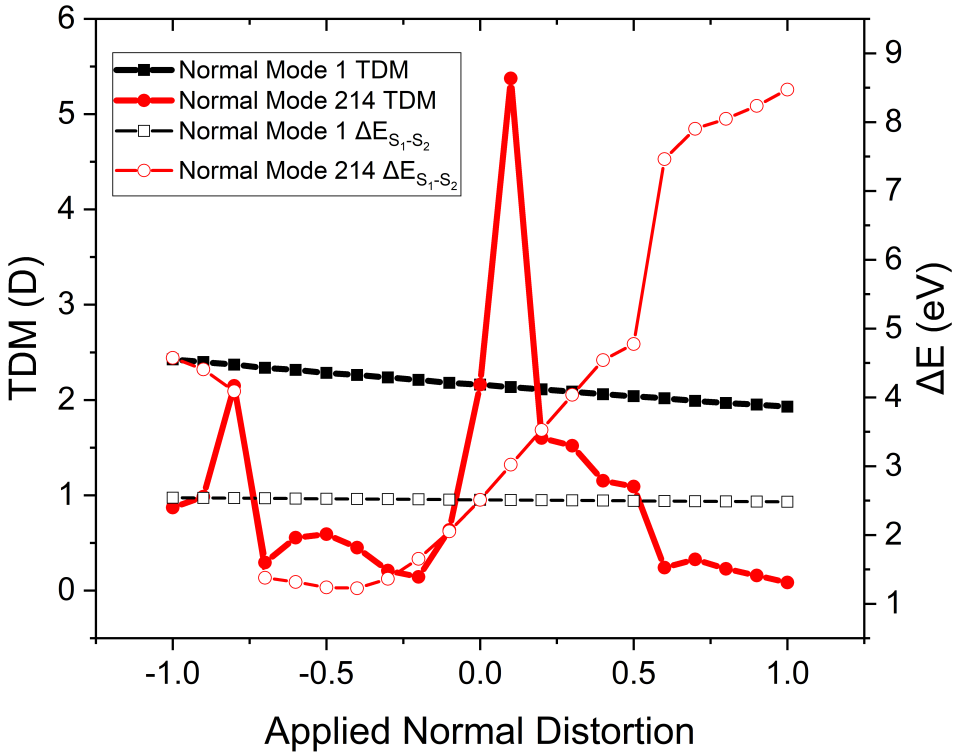

Fig. 13 Normal Mode scan along modes 1 and 214, with a double y axis showing the S1 TDM change and the single HOMO-LUMO contribution to S1 along applied normal distortion.

7 Calculating the S_1 Spectral Lineshape

Computing S_1 absorption directly from the MD spectral density results in an unphysically broad and vibronically featureless (Supp. Fig. 14 **B** inset), that is almost entirely buried under the S_2 line. Due to the lack of oscillator strength is has a negligible amplitude. If we correct for the over-estimate in the S_1 vibronic coupling (by assuming S_1 has the same vibronic structure as S_2) we get the corrected lineshape shown in Supp. Fig. 14 **C** (inset). This over-estimate is actually useful as it means that the marginal effects of geometry distortions revealed by our calculation are actually themselves over-estimates.

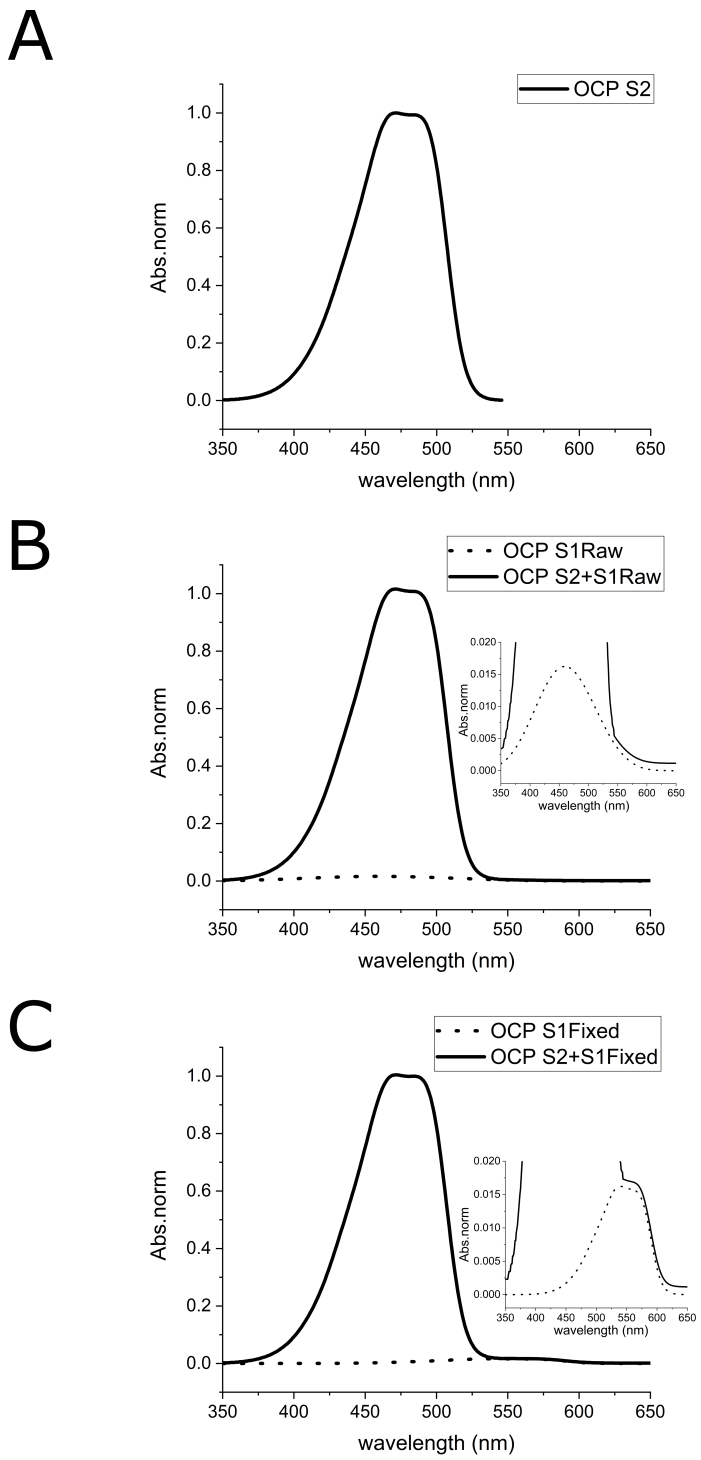

Fig. 14 A. Calculated S_2 absorption spectrum of Ech in OCP$_o$. **B.** Calculated OCP$_o$ absorption spectrum including the negligible absorption from S_1. Here the S_1 line shape is calculate directly from the MD trace without any correction of the over-estimate of the vibronic coupling. The S_1 lineshape is shown in detail in the inset. **C.** Calculated OCP$_o$ absorption spectrum in which the over-estimate of the S_1 vibronic coupling has been corrected.

References

1 I. G. Prandi, L. Viani, O. Andreussi and B. Mennucci, *J Comput. Chem.*, 2016, **37**, 981–991.